Chemistry & Biology, Vol. 10, 149–159, February, 2003, ©2003 Elsevier Science Ltd. All rights reserved. DOI 10.1016/S1074-5521(03)00022-X

Conformational Restriction via Cyclization in β-Amyloid Peptide Aβ(1-28) Leads to an Inhibitor of Aβ(1-28) Amyloidogenesis and Cytotoxicity

Aphrodite Kapurniotu,[1,*] Andreas Buck,[1] Marco Weber,[1] Anke Schmauder,[1] Thomas Hirsch,[1] Jürgen Bernhagen,[2] and Marianna Tatarek-Nossol[1,2]

[1]Laboratory of Bioorganic and Medicinal Chemistry
[2]Department of Biochemistry
and Molecular Cell Biology
Institute of Biochemistry
University Hospital of the RWTH Aachen
D-52074 Aachen
Germany

Summary

The aggregation process of β-amyloid peptide Aβ into amyloid is strongly associated with the pathology of Alzheimer's disease (AD). Aggregation may involve a transition of an α helix in Aβ(1-28) into β sheets and interactions between residues 18–20 of the "Aβ amyloid core." We applied an i, i+4 cyclic conformational constraint to the Aβ amyloid core and devised side chain-to-side chain lactam-bridged cyclo$^{17, 21}$-[Lys^{17}, Asp^{21}]Aβ(1-28). In contrast to Aβ(1-28) and [Lys^{17}, Asp^{21}] Aβ(1-28), cyclo$^{17, 21}$-[Lys^{17}, Asp^{21}]Aβ(1-28) was not able to form β sheets and cytotoxic amyloid aggregates. Cyclo$^{17, 21}$-[Lys^{17}, Asp^{21}]Aβ(1-28) was able to interact with Aβ(1-28) and to inhibit amyloid formation and cytotoxicity. Cyclo$^{17, 21}$-[Lys^{17}, Asp^{21}]Aβ(1-28) also interacted with Aβ(1-40) and interfered with its amyloidogenesis. Cyclo$^{17, 21}$-[Lys^{17}, Asp^{21}]Aβ(1-28) or similarly constrained Aβ sequences may find therapeutic and diagnostic applications in AD.

Introduction

One of the main features of Alzheimer's disease (AD) comprises deposition of extracellular plaques and associated neuronal injury in the brains of AD patients [1]. The plaques consist of amyloid fibrils of the β-amyloid peptide (Aβ) which is a 40 (Aβ(1-40)) to 42 (Aβ(1-42)) amino acid long peptide [1, 2]. The soluble monomeric form of Aβ is present under both normal and disease conditions in the cerebrospinal fluid (CSF) and blood [3]. However, aggregation of Aβ into amyloid has been strongly associated with the pathological sequelae of AD [1, 4]. One reason for this is that Aβ oligo- and multimeric aggegates, contrary to monomeric Aβ, exhibit cytotoxic and neurotoxic effects [5–10].

Several Aβ aggregation and amyloid formation inhibitory approaches have been investigated over the past 10 years [11–17]. Aβ amyloidogenesis has been suggested to proceed via a conformational transition of monomeric Aβ into β sheet aggregates [18–22]. Inhibition of β sheet formation via introduction of β sheet-"breaking" residues [12, 13, 16, 17, 23] or sequences [14, 24] in short amyloid core-containing Aβ sequences has resulted in inhibitors or modulators of Aβ amyloidogenesis and cytotoxicity.

In this work, a strategy to "transform" an amyloidogenic sequence into a nonamyloidogenic one that is able to interact with the native amyloid-forming sequence and inhibit amyloid formation and cytotoxicity was tested on the N-terminal Aβ sequence Aβ(1-28). According to the design approach, a sequence part of Aβ that may be directly involved in the transition of a potential α-helical state into β sheets and in Aβ-Aβ self-recognition and self-assembly [17–19, 21, 25–31] was conformationally constrained into an non-β state via side chain-to-side chain cyclization. We present the design and study of the biochemical and biophysical properties of the cyclic analog, its ability to inhibit amyloid formation and cytotoxicity of Aβ(1-28), and its interference with Aβ(1-40) amyloidogenesis.

Results

Analog Design

The mechanism of the conformational transition of monomeric Aβ into amyloid is not yet known. Proposed mechanisms include a transition of a potential α helix in the N-terminal sequence Aβ(1-28) into aggregated β sheets [18, 19, 21, 25], possibly via α-helical oligomers [32], and amyloidogenesis via a collapsed coil conformation [31]. Aβ(1-28) is a conformationally flexible sequence that has been proposed to exist in an α-helical state or as β sheet-containing amyloid aggregates [18, 19, 21, 25, 33, 34]. Aβ(1-28) amyloid fibrils are indistinguishable from Aβ fibrils [33, 35]. Because the transition of Aβ(1-28) into β sheets has been proposed to modulate Aβ amyloidogenesis, this sequence has been often applied as a model peptide for Aβ [18–21, 25, 33, 34, 36, 37]. Although it is clear that Aβ(1-28) per se does not correspond to a physiologically relevant sequence for AD, its use as a model sequence for Aβ should assist in understanding the mechanism and the development of inhibitors of amyloidogenesis and related cytotoxicity.

To constrain Aβ(1-28) in a non-β conformation, we applied the i, i+4 side chain-to-side chain cyclization approach, and a Lys^{i}, Asp^{i+4} pair was used to generate the lactam-bridged analog cyclo$^{17, 21}$-[Lys^{17}, Asp^{21}]Aβ(1-28) (Figure 1, scheme) [38–40]. The Lys^{17}, Asp^{21} pair was chosen because such a bridge has previously been shown to be able to stabilize the α-helical conformation in conformationally flexible polypeptides [40–44]. As to the complexity of the synthesis of the compound, it may have been simpler to constrain peptide conformation through a Cys, Cys bridge [45]. As the bridge was to be introduced into Aβ, which is a highly aggregation-prone sequence, we chose to use a lactam bridge instead of a disulfide bridge due to the various conformational and chemical factors that may determine formation and stability of a disulfide bridge and the susceptibility of free thiol-containing sequences to aggregation [46, 47].

*Correspondence: akapurniotu@ukaachen.de

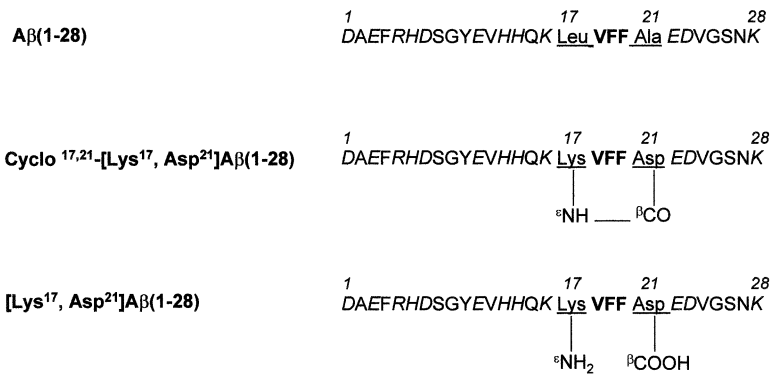

Figure 1. Scheme Showing Primary Structure of Aβ(1-28), Cyclo^{17,21}-[Lys^{17}, Asp^{21}]Aβ(1-28), and [Lys^{17}, Asp^{21}]Aβ(1-28)

Residues of the "Aβ-Aβ self-recognition" sequence 18–20 are in bold. Charged residues are written in italics. Residues Leu^{17} and Ala^{21} that were substituted by Lys and Asp, respectively, are underlined. The one-letter code is used for the amino acids with the exception for residues 17 and 21. The lactam bridge in cyclo^{17,21}-[Lys^{17}, Asp^{21}]Aβ(1-28) and the functional groups of the side chains of Lys^{17} and Asp^{21} in [Lys^{17}, Asp^{21}]Aβ(1-28) are also shown.

The lactam-bridged residues were placed at positions 17 and 21 because it has been proposed that the Aβ amyloid formation process might be associated with an unfolding of a helix between residues 13 and 20 [21, 25, 34]. We hypothesized that stabilization of this part of the helix might inhibit amyloidogenesis. A second reason was that it has been suggested that interactions of the side chains of the hydrophobic residues Val^{18}, Phe^{19}, and Phe^{20} might directly contribute to Aβ self-association with sequence (18–20) serving as an "Aβ-Aβ self-recognition" sequence [17, 21, 23, 26, 28–31]. Therefore, the amino acid constitution of sequence (18–20) should be kept intact to enable for the interaction with Aβ to occur and should become conformationally constrained, which would render the analog unable to form extended β sheets as in fibrillar aggregates [26]. To differentiate the effects of constraining the conformation via cyclization from potential effects of the substituents themselves, [Lys^{17}, Asp^{21}]Aβ(1-28) was also studied.

AFM, CR Binding, and FT-IR Studies on the β Sheet-Forming and Amyloidogenic Properties of Aβ(1-28) and Cyclo^{17,21}-[Lys^{17}, Asp^{21}]Aβ(1-28)

The amyloidogenic and β sheet-forming potentials were first studied using highly concentrated (1 mM) solutions of the synthetic peptides aged for 2 months at 4°C. Such aging conditions appear rather extreme. However, these conditions or conditions similar to those used here have often been applied to simulate in vitro conditions of local supersaturation that may lead to in vivo amyloid formation [23, 30, 33, 48–51]. Denaturating electrophoresis (NuPAGE), reverse phase high-pressure liquid chromatography (RP-HPLC), and mass spectroscopic (MALDI-MS) analyses of the aged solutions suggested that no peptide degradation had occurred (data not shown).

Atomic force microscopy (AFM) showed that aged Aβ(1-28) predominantly consisted of long amyloid fibrils (1–8 μm) and wound fibrillar bundles with diameters of 7–13 nm and an axial periodicity of ~28 nm [33, 52] (Figure 2A). No amyloid fibrils were detected in aged cyclo^{17,21}-[Lys^{17}, Asp^{21}]Aβ(1-28) (Figure 2D). Aβ(1-28) also bound congo red (CR) and exhibited green/yellow birefringence under polarized light characteristic for amyloid [53] (Figure 2B). On the contrary, cyclo^{17,21}-[Lys^{17}, Asp^{21}]Aβ(1-28) did not exhibit any birefringence (Figure 2E). The Fourier-transformed infra red (FT-IR) spectrum of Aβ(1-28) (Figure 2A) exhibited a sharp absorbance maximum at 1627 cm^{-1} (Figure 2C) that is usually assigned to β sheet [33, 35, 54]. By contrast, the spectrum of cyclo^{17,21}-[Lys^{17}, Asp^{21}]Aβ(1-28) had a broad absorbance maximum at 1650–1670 cm^{-1} and indicated that non-β conformations were predominant [54].

CD and EM Studies on the β Sheet-Forming Potential and Amyloidogenicity of Cyclo^{17,21}-[Lys^{17}, Asp^{21}]Aβ(1-28), Aβ(1-28)

The transition of soluble Aβ(1-28) into amyloid was followed by circular dichroism (CD) spectroscopy and electron microscopy (EM) under amyloidogenesis-promoting conditions. As shown in Figure 3A, Aβ(1-28) was in a mainly disordered state mixed with some ordered elements at the beginning of the aging process [55]. The spectrum did not change over the next 17 hr, and EM showed a complete absence of fibrillar aggregates (data not shown). Then, the shape and position of the minimum of the spectra changed and a time-dependent red shift of the minimum from 202 nm (between 0 and 17 hr) to 208 nm (at a time point of about 21 hr) was observed. The shift was indicative of the formation of significant amounts of more ordered conformeric populations [55]. The conformational transition of Aβ(1-28) was completed at 25 hr (Figures 3A and 3B): the spectrum had a strong minimum at 220 nm that suggested that β sheet was the predominant conformeric state [49, 55], and insoluble aggregates appeared. EM showed that the aggregates consisted predominantly of fibrils (Figure 3B).

The ability of cyclo^{17,21}-[Lys^{17}, Asp^{21}]Aβ(1-28) to aggregate into β sheets and amyloid was studied next. Figure 3C shows the CD spectra of a solution of cyclo^{17,21}-[Lys^{17}, Asp^{21}]Aβ(1-28) immediately following the beginning of the incubation and 8 days later. No changes were observed during the 8 day period. The spectrum of cyclo^{17,21}-[Lys^{17}, Asp^{21}]Aβ(1-28) had minima at 206 nm and in the region of 220–225 nm and was indicative of mixtures of random coil with significant amounts of ordered populations [55]. No amyloid assemblies were detected by EM during the aging process (Figure 3D).

Studies on the β Sheet and Amyloid-Forming Potential of [Lys^{17}, Asp^{21}]Aβ(1-28)

FT-IR, CR staining, and EM showed that [Lys^{17}, Asp^{21}]Aβ(1-28) had, similarly to Aβ(1-28), both a pro-

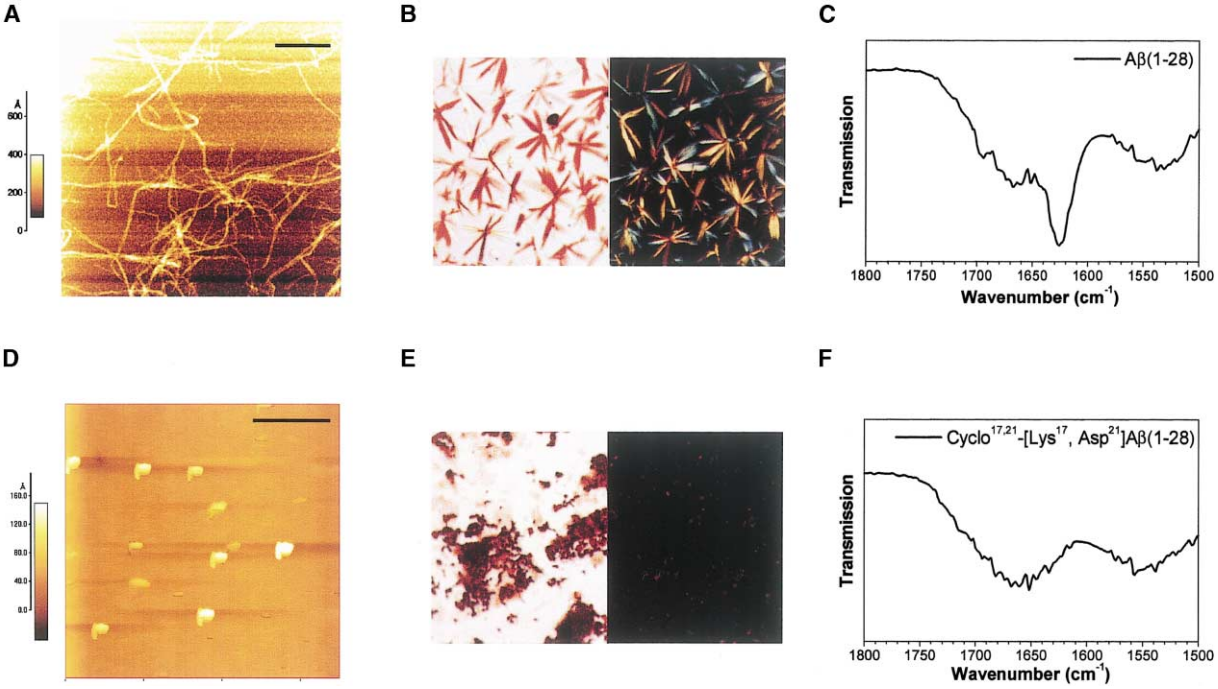

Figure 2. Amyloidogenic and β Sheet-Forming Potentials of Aβ(1-28) versus Cyclo^{17,21}-[Lys^{17}, Asp^{21}]Aβ(1-28) as Assessed by AFM, CR Staining and Polarization Microscopy, and FT-IR

(A) AFM image (10 × 10 μm; bar 2 μm) of aged Aβ(1-28).

(B) Microscopic examination of aged Aβ(1-28) following CR staining under normal field (on the left) and under polarized light (on the right).

(C) FT-IR spectrum of aged Aβ(1-28).

(D) AFM image (7 × 7 μm; bar, 2 μm) of aged cyclo^{17,21}-[Lys^{17}, Asp^{21}]Aβ(1-28).

(E) Microscopic examination of aged cyclo^{17,21}-[Lys^{17}, Asp^{21}]Aβ(1-28) following CR staining under normal field (on the left) and under polarized light (on the right).

(F) FT-IR spectum of aged cyclo^{17,21}-[Lys^{17}, Asp^{21}]Aβ(1-28).

nounced β sheet-forming potential (FT-IR absorbance maximum was at 1627 cm^{-1}) and strong amyloidogenic properties (data not shown). CD showed that aging of [Lys^{17}, Asp^{21}]Aβ(1-28) resulted in a conformational transition into β sheets and insoluble aggregates (data not shown). EM showed that the aggregates consisted of amyloid fibrils that were indistinguishable from those of Aβ(1-28) [33, 35, 52].

CD Studies on the α-Helical Propensity of Cyclo^{17,21}-[Lys^{17}, Asp^{21}]Aβ(1-28)

CD spectra of Aβ(1-28) and cyclo^{17,21}-[Lys^{17}, Asp^{21}]Aβ(1-28) were measured under nonamyloidogenic and very weak helix-promoting conditions [18, 19, 21, 35] (Figure 4). The spectrum of Aβ(1-28) exhibited a minimum at 205 nm and indicated the presence of significant amounts of random coil mixed with other ordered elements [55] (Figure 4). Of note, this spectrum was very similar to the one that has previously been obtained by Barrow et al. [19]. The spectrum of [Lys^{17}, Asp^{21}]Aβ(1-28) was very similar to that of Aβ(1-28) (Figure 4). By contrast, the spectrum of cyclo^{17,21}-[Lys^{17}, Asp^{21}]Aβ(1-28) had a maximum at 195 nm and two pronounced minima at 208 and 222 nm (Figure 4), consistent with the presence of higher amounts of α-helical structure in the cyclic analog than in Aβ(1-28) and [Lys^{17}, Asp^{21}]Aβ(1-28) [55].

CD, EM, Size Exclusion Chromatography, and Cell Viability Studies on the Interaction and the Inhibitory Effect of Cyclo^{17,21}-[Lys^{17}, Asp^{21}]Aβ(1-28) on β Sheet, Amyloid Formation, and Cytotoxicity of Aβ(1-28)

Incubations of a mixture of cyclo^{17,21}-[Lys^{17}, Asp^{21}]Aβ(1-28) with Aβ(1-28) were performed, and the effect of aging on conformation and amyloid formation was followed at various time points in parallel by CD (Figure 5A) and EM (Figure 5C). The spectrum of the mixture did not change over 8 days, corresponding to the time range of the CD study, and the solution remained clear. The spectrum of the mixture strongly differed from that corresponding to the mathematical sum of the CD spectra of each of the mixture components alone (Figure 5A). This indicated that the two peptides might have interacted [56]. No amyloid fibrils could be detected by EM (Figure 5C) not only at the time point of 8 days but also up to 3 weeks. By contrast, aggregation of Aβ(1-28) alone into β sheets (Figure 3A) and amyloid (Figure 3B), even at half of the concentration applied in the mixing experiment, was accomplished already at 25 hr of aging, while, at the same concentration as that applied in the mixture, Aβ(1-28) aggregated into amyloid between 2 and 6 hr (Figure 5B). In another series of experiments, cyclo^{17,21}-[Lys^{17}, Asp^{21}]Aβ(1-28) was also found to inter-

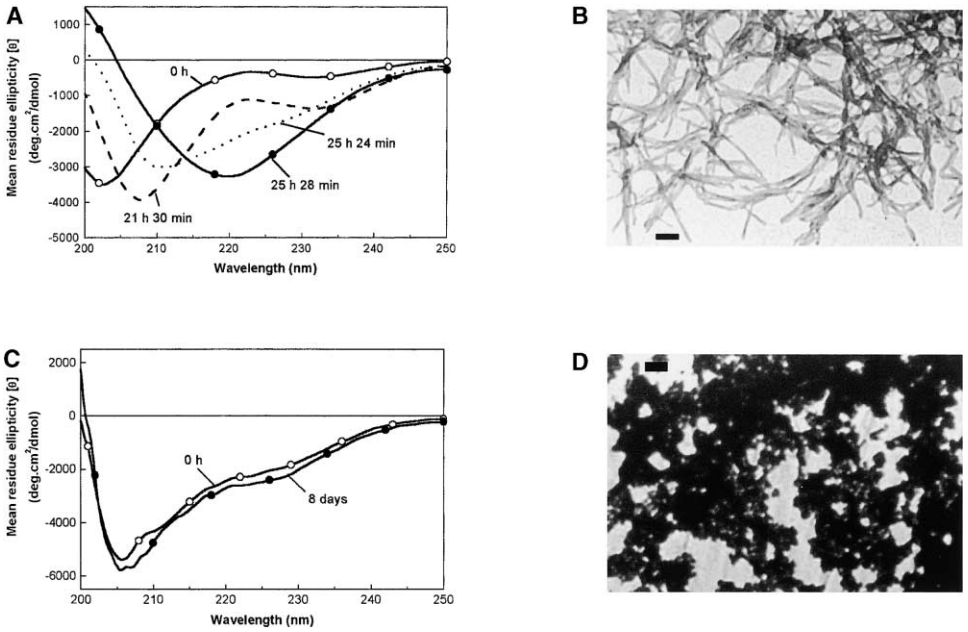

Figure 3. Conformational Transitions in the Process of Amyloid Formation by Aβ(1-28) versus Cyclo$^{17, 21}$-[Lys^{17}, Asp^{21}]Aβ(1-28) as Assessed by CD and EM

(A) Far-UV CD spectra of Aβ(1-28) (225 μM) at time 0 hr after beginning the incubation and at the indicated time points thereafter.

(B) Electron micrograph of the Aβ(1-28) solution shown under (A) at the time point of 25 hr and 30 min.

(C) Far-UV CD spectra of cyclo$^{17, 21}$-[Lys^{17}, Asp^{21}]Aβ(1-28) (450 μM) at time 0 hr after beginning the incubation and 8 days thereafter.

(D) Electron micrograph of a solution of cyclo$^{17, 21}$-[Lys^{17}, Asp^{21}]Aβ(1-28) (450 μM; see [C]) 8 days following the beginning of incubation. Bars in the electron micrographs represent 100 nm.

act with and completely block amyloid formation by [Lys^{17}, Asp^{21}]Aβ(1-28) (data not shown).

We next studied the effects of aged solutions of Aβ(1-28), cyclo$^{17, 21}$-[Lys^{17}, Asp^{21}]Aβ(1-28) and of a mixture of Aβ(1-28) with cyclo$^{17, 21}$-[Lys^{17}, Asp^{21}]Aβ(1-28) on the viability of a human glioblastoma/astrocytoma cell line [56]. EM showed that aged Aβ(1-28) mainly consisted of amyloid aggregates (Figure 5B), whereas cyclo$^{17, 21}$-[Lys^{17}, Asp^{21}]Aβ(1-28) and the mixture did not contain amyloid (Figures 3D and 5C). Following incubation with the cells at peptide concentrations of 10 and 5 μM, the MTT reduction assay was used to assess the effect of the peptides on cell viability. This assay is based on the cellular reduction of the dye 3-[4,5-dimethylthiazol-2-yl]-2,5-diphenyltetrazolium bromide (MTT), which is an indicator of cellular redox activity [5]. Aβ and other amyloid-forming peptides have been shown to decrease cellular redox activity. Redox activity is closely associated with cell viability [5, 6, 8, 14, 16, 51, 56]. Based on this assay, the solution containing Aβ(1-28) amyloid aggregates was cytotoxic to HTB14 cells (Figure 5D). By contrast, cell viability was significantly increased in cells treated with cyclo$^{17, 21}$-[Lys^{17}, Asp^{21}] Aβ(1-28) alone and with the mixture of cyclo$^{17, 21}$-[Lys^{17}, Asp^{21}]Aβ(1-28) with Aβ(1-28) (Figure 5D).

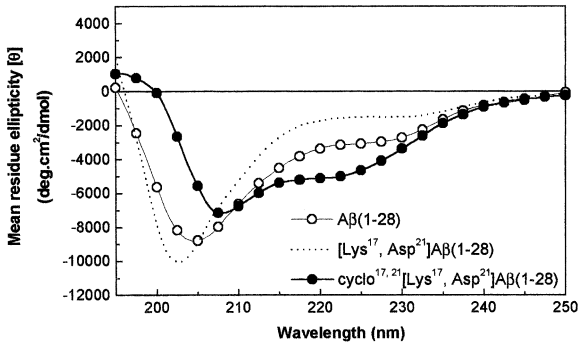

Figure 4. α-Helical Propensities of Cyclo$^{17, 21}$-[Lys^{17}, Asp^{21}]Aβ(1-28), Aβ(1-28), and [Lys^{17}, Asp^{21}]Aβ(1-28) as Assessed by Far-UV CD

We next followed the aggregation of Aβ(1-28), cyclo$^{17, 21}$-[Lys^{17}, Asp^{21}]Aβ(1-28), and of a mixture of both peptides using size exclusion chromatography (Figures 6A–6D). The main peak of Aβ(1-28) (at 22.6 min) immediately after beginning the incubation corresponded to dimeric Aβ(1-28). NuPAGE analysis also indicated that Aβ(1-28) had a strong dimerization propensity (data not shown). During the 5 days of incubation, the amount of Aβ(1-28) dimers rapidly decreased and an increase in high molecular weight aggregates that were eluted in the void volume of the column (12 min) was observed (Figures 6E and 6F). Aggregation of Aβ(1-28) was nearly completed at 5 days (Figure 6D). Cyclo$^{17, 21}$-[Lys^{17}, Asp^{21}] Aβ(1-28) appeared to have a similar dimerization and aggregation propensity as Aβ(1-28) (Figures 6A–6D). Of note, the cyclic analog was very strongly retained on the column, which might be due to a strong surface exposure of the hydrophobic amyloid core sequence 18–20 due to the cyclic constraint. In the mixture of Aβ(1-28) with cyclo$^{17, 21}$-[Lys^{17}, Asp^{21}]Aβ(1-28), dimers were also the main oligomeric forms present. The decrease of the amount of dimers in the mixture was,

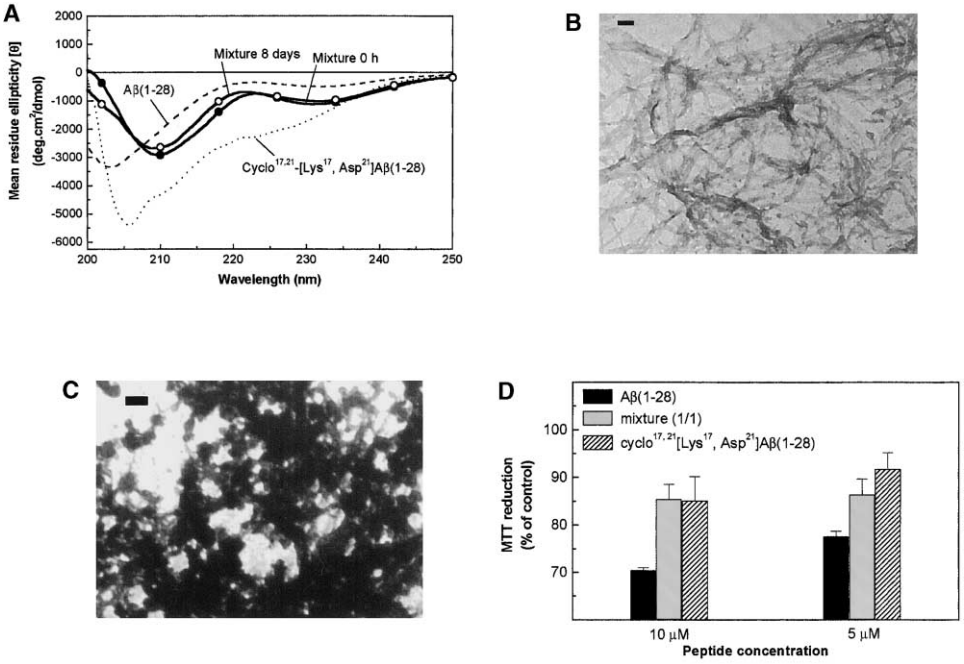

Figure 5. Inhibitory Effect of Cyclo[17, 21]-[Lys[17], Asp[21]]Aβ(1-28) on Amyloid Formation and Cytotoxicity of Aβ(1-28) as Assessed by Far-UV CD, EM, and the MTT Cell Viability Assay

(A) CD spectra of a mixture of Aβ(1-28) and cyclo[17, 21]-[Lys[17], Asp[21]]Aβ(1-28) (450 μM each) at 0 hr and 8 days following the begin of incubation. CD spectra of Aβ(1-28) (450 μM) alone at the beginning of an incubation and of cyclo[17, 21]-[Lys[17], Asp[21]]Aβ(1-28) alone (450 μM) are also shown.

(B) Electron micrograph of aged Aβ(1-28) (450 μM, see [A]) at 4 days.

(C) Electron micrograph of the aged mixture of Aβ(1-28) with cyclo[17, 21]-[Lys[17], Asp[21]]Aβ(1-28) (450 μM each, see [A]) 5 days upon making the mixture. Bars in the electron micrographs represent 100 nm.

(D) Cell viability in the presence of aged Aβ(1-28) alone, cyclo[17, 21]-[Lys[17], Asp[21]]Aβ(1-28) alone, and a mixture of Aβ(1-28) with cyclo[17, 21]-[Lys[17], Asp[21]]Aβ(1-28). Data are percentages of control values (vehicle alone) and are the mean ± SD of four to five determinations.

however, much slower than in Aβ(1-28) alone (Figure 6), and only very low amounts of high molecular weight aggregates formed. This data indicated that interaction of cyclo[17, 21]-[Lys[17], Asp[21]]Aβ(1-28) with Aβ(1-28) might have resulted in formation of heterodimers that were more resistant to further aggregation than Aβ(1-28) dimers and/or that the cyclic analog might have caused a dissociation of high molecular weight aggregates. A small fraction of Aβ(1-28) in the incubation of Aβ(1-28) alone eluted as a monomer (at 27 min), and its amount did not change during the incubation time. By contrast, the fraction of monomeric peptide significantly increased during the incubation of the mixture (Figures 6A–6D). This indicated that interaction of the cyclic analog with Aβ(1-28) might also have resulted in a dissociation of dimeric or multimeric Aβ(1-28) into monomers.

Studies on the Interaction of Cyclo[17, 21]-[Lys[17], Asp[21]]Aβ(1-28) with Aβ(1-40)

To investigate the ability of cyclo[17, 21]-[Lys[17], Asp[21]] Aβ(1-28) to bind Aβ(1-40), we established an Aβ(1-40) pull-down assay [57] in combination with NuPAGE gel electrophoresis and Western blotting with an anti-Aβ(1-40) antibody (Figure 7A). Complexes of the cyclic peptide and its potential interaction partner Aβ(1-40) were isolated via binding of the biotinylated cyclic peptide on streptavidin-coated magnetic beads, the subsequent dissociation of these complexes from the beads, and, finally, by revealing the components of the complexes by Western blotting against Aβ(1-40) (by antibody) (Figure 7A, left panel) and by NuPAGE in combination with an anti-streptavidin antibody to reveal the biotinylated complex component (Figure 7A, right panel). The anti-Aβ(1-40) Western blot showed that the retrieved amount of Aβ(1-40) in the mixture with the cyclic peptide was at least twice as high as that obtained for Aβ(1-40) due to nonspecific binding to the beads (Figure 7A, left panel). This result suggested that cyclo[17, 21]-[Lys[17], Asp[21]] Aβ(1-28) was able to bind Aβ(1-40).

Thioflavin T (ThT) binding to amyloid and the associated increase in ThT fluorescence emission is used as a specific assay for the detection of amyloid aggregates [58]. Aged solutions of Aβ(1-40) showed a significantly increased ThT fluorescence emission as compared to solutions containing a mixture of Aβ(1-40) with the cyclic analog, and no increase in ThT fluorescence was observed in cyclo[17, 21]-[Lys[17], Asp[21]]Aβ(1-28) alone (data not shown). These results indicated that the cyclic peptide interfered with the amyloid formation process of Aβ(1-40) and prompted us to undertake EM studies.

In fact, further evidence for the interference of cyclo[17, 21]-[Lys[17], Asp[21]]Aβ(1-28) with the amyloidogenesis process of Aβ(1-40) was obtained by EM. Aged Aβ(1-40) predominantly contained fibrils with diameters of 6–10 nm and of indefinite lengths (Figure 7B), i.e., typical values for "mature" amyloid. By contrast, solu-

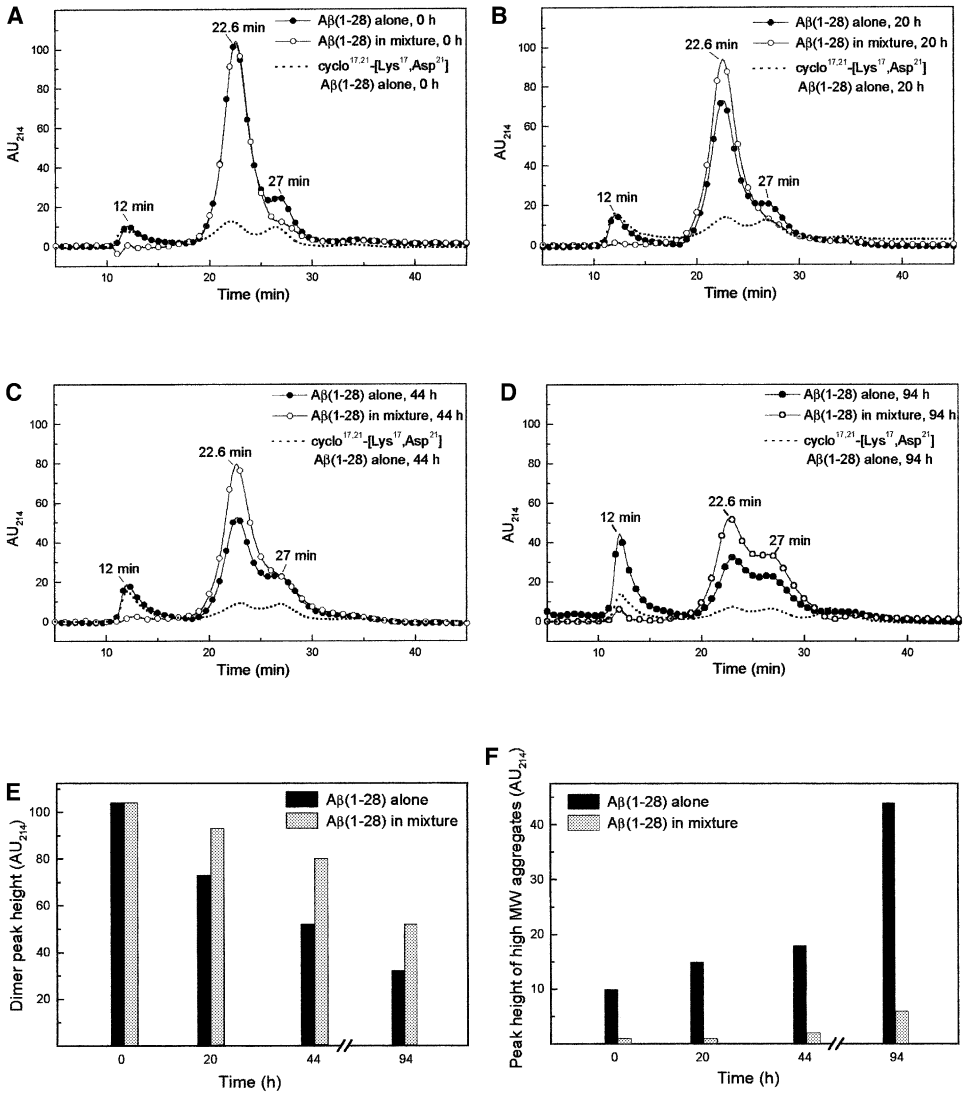

Figure 6. Interaction of Cyclo^{17,21}-[Lys^{17}, Asp^{21}]Aβ(1-28) with Aβ(1-28) and Inhibition of the Aggregation of Aβ(1-28) as Followed by Size Exclusion Chromatography at Different Time Points

Aβ(1-28) alone, cyclo^{17,21}-[Lys^{17}, Asp^{21}]Aβ(1-28) alone, and a mixture of Aβ(1-28) with cyclo^{17,21}-[Lys^{17}, Asp^{21}]Aβ(1-28) were aged for 5 days at room temperature.

(A–D) Chromatograms at various time points including the time points 0 hr (A), 20 hr (B), 44 hr (C), and 94 hr (D) are shown. Retention times are indicated on the chromatograms. The chromatogram of cyclo^{17,21}-[Lys^{17}, Asp^{21}]Aβ(1-28) was subtracted from the chromatogram of the mixture.

(E and F) Kinetics of Aβ(1-28) aggregation alone versus in the mixture are shown. Amounts of Aβ(1-28) dimers (E) and high molecular weight aggregates (F) in both solutions as indicated are plotted versus time. Results shown represent results from two independent experiments.

tions of a mixture of Aβ(1-40) with the cyclic analog consisted of three populations of aggregates: one population (less than 10% of the total) was similar to the above described fibrils (Figure 7C), a second population (20%–30%) consisted of short (<200 nm) fibrils (Figure 7D) that were strongly reminiscent of the protofibrillar Aβ(1-40) species that have been previously described [22], and a third population consisted of amorphous aggregates (Figure 7E) and corresponded to a major aggregate population.

Discussion

Cyclo^{17,21}-[Lys^{17}, Asp^{21}]Aβ(1-28) was unable to form β sheets and amyloid aggregates. This could be attributed to the effect of the conformational constraint as compared to the substituents alone. Cyclo^{17,21}-[Lys^{17}, Asp^{21}] Aβ(1-28) was also able to self-associate into soluble, oligo- and high molecular weight amorphous aggregates. These findings suggest that the conformation that was stabilized in Aβ(1-28) by the cyclic constraint is

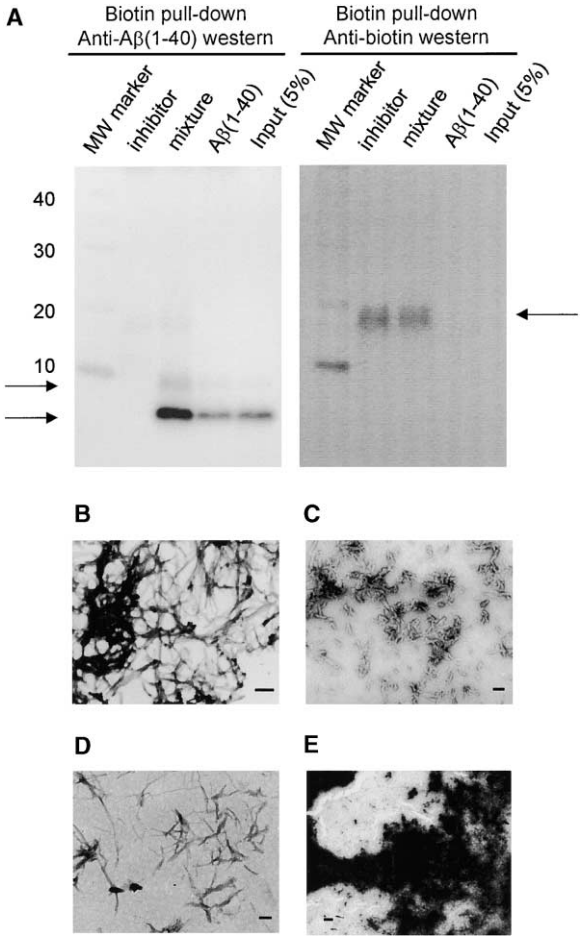

Figure 7. Interaction of Cyclo$^{17, 21}$-[Lys^{17}, Asp^{21}]Aβ(1-28) with Aβ(1-40) and the Effect on Amyloidogenesis as Assessed by a Binding Assay and EM

(A) Left panel, anti-Aβ(1-40) Western blot analysis following pull down of N$^{\alpha}$-biotinyl-cyclo$^{17, 21}$-[Aca^{0}, Lys^{17}, Asp^{21}]Aβ(1-28)/Aβ(1-40) complexes. Lane, inhibitor: N$^{\alpha}$-biotinyl-cyclo$^{17, 21}$-[Aca^{0}, Lys^{17}, Asp^{21}] Aβ(1-28) alone; lane, mixture: complex-bound Aβ(1-40); lane, Aβ(1-40): Aβ-(1-40) alone was incubated with beads (nonspecific binding); lane, input (5%): 5% freshly dissolved Aβ(1-40) (0.5 μg) (not incubated with the beads). Nonspecific binding was thus less than 5% of total Aβ(1-40). Arrows indicate detected monomers and dimers of Aβ(1-40). Right panel, identical samples were subjected to the pull-down procedure, and the blot was revealed with streptavidin-POD. Arrow indicates N$^{\alpha}$-biotinyl-cyclo$^{17, 21}$-[Aca^{0}, Lys^{17}, Asp^{21}]Aβ(1-28) oligomers.

(B) Electron micrographs of aged Aβ(1-40) (46 μM) 7 days following incubation begin.

(C–E) Electron micrographs of aggregates formed in an aged mixture of Aβ(1-40) (46 μM) with cyclo$^{17, 21}$-[Lys^{17}, Asp^{21}]Aβ(1-28) (60 μM) at 7 days.

compatible with the high-self-association propensity of Aβ(1-28) but is incompatible with the potential of Aβ(1-28) to aggregate into β sheets and amyloid fibrils. These findings support the suggestion that a conformational transition into β sheets is a necessary step in Aβ amyloidogenesis [59], and additionally support the idea that the self-recognition ability of Aβ(1-28) and its ability to self-associate into amorphous (i.e., nonamyloid) aggregates are not necessarily associated with its β sheet-forming ability. CD studies indicated that cyclo$^{17, 21}$-[Lys^{17}, Asp^{21}]Aβ(1-28) may have a higher α helix-forming propensity than Aβ(1-28). Thus, although NMR studies are now necessary to determine the precise conformation of the cyclic analog, our findings are consistent with the suggestion that an α helix to β sheet transition is an important step in Aβ(1-28) amyloidogenesis [18, 19, 21, 25].

According to the MTT reduction assay, aged Aβ(1-28) affected cellular redox activity and thus viability of a human astroglioma/astrocytoma cell line [56, 60]. By contrast, cyclo$^{17, 21}$-[Lys^{17}, Asp^{21}]Aβ(1-28) was markedly less cytotoxic. It should however be noted that, because cellular redox ability is only one parameter of cell viability and amyloid-mediated cell damage [5, 6, 8], additional assays will be necessary to understand the effect of these peptides on cells. Blocking the amyloidogenic potential and, in some cases, also cytotoxicity of partial Aβ sequences by means of substituting crucial amyloid core residues or by N-methylation of amide bonds in the amyloid core region has previously been reported [12, 16, 23, 28, 30]. Also, Esler et al. [59] have recently shown that an Aβ(10-35) congener that had a high-energy barrier to a conformational transition did not deposit into amyloid. The results of our work support the above findings and show for the first time that the direct conformational restriction of an amyloid core sequence via cyclization may result in inhibition of both the amyloid-forming and the cytotoxic potential of the native sequence.

Importantly, cyclo$^{17, 21}$-[Lys^{17}, Asp^{21}]Aβ(1-28) was able to interact with Aβ(1-28) and to inhibit its aggregation into amyloid and its cytotoxic effect. These results are consistent with findings that interference with and/or inhibition of Aβ aggregation into amyloid may result in an inhibition of amyloid-related cytotoxicity [12–14, 16]. Size exclusion chromatography indicated that interaction of the cyclic peptide with Aβ(1-28) and thus the observed inhibitory effect on Aβ(1-28) aggregation into amyloid might include formation of heterodimers and/or a dissociation of Aβ(1-28) oligomers and multimers. CD suggested that the above interaction was associated with conformational changes. Association of the cyclic and, potentially, α helix-stabilized Aβ(1-28) analog with Aβ(1-28) might have led to an assembly that may not be able to convert into amyloid fibrils due to the constraint in the analog. In that way, Aβ(1-28) would have been sequestered from the amyloid formation pathway. Such an assembly might consist of oligomeric α helices. Formation of α-helical oligomeric assemblies has recently been proposed to be a key on- or off-pathway step in Aβ(1-40) fibrillogenesis [22, 32]. A similar mechanism of interaction has been proposed to account for the inhibitory activity of side chain lactam-bridged and α helix-stabilized peptides on HIV type 1 infectivity [61].

Although our studies use the nonnative fragment Aβ(1-28) as a model peptide for Aβ, it may be derived from the results obtained on the interaction of cyclo$^{17, 21}$-[Lys^{17}, Asp^{21}]Aβ(1-28) with Aβ(1-40) that they are biologically relevant. In fact, the cyclic analog was also found to be capable of binding Aβ(1-40). In addition, while

this peptide did not inhibit aggregation of Aβ(1-40) into "mature" amyloid fibrils, it was able to interfere with the process of amyloidogenesis. Our data indicate that interference was related to formation or stabilization of short fibrillar Aβ(1-40) aggregates that appeared to be similar to protofibrillar Aβ(1-40) [22, 62]. A detailed characterization of the effect of the cyclic analog on amyloidogenesis and cytotoxicity of Aβ(1-40) should assist in elucidation of mediators of cytotoxicity, i.e., fibrils versus protofibrils and other aggregates [9, 10, 63].

Our study suggests that, by introducing a rationally designed conformational constraint into an amyloid core sequence and at the same time maintaining some of the sequence-specific self-assembly determinants, it is possible to convert a native amyloidogenic sequence into a nonamyloidogenic one which is able to interact with the native sequence and inhibit or interfere with its amyloidogenesis pathway and cytotoxic effects.

Significance

The conformational transition of Aβ into β sheet-containing amyloid is strongly associated with the pathogenesis of AD. Here, we have applied an i, i+4 side chain lactam bridge conformational constraint to the amyloid core sequence 18–20 of the amyloidogenic N-terminal Aβ sequence Aβ(1-28). In contrast to Aβ(1-28), the cyclic analog cyclo^{17,21}-[Lys^{17}, Asp^{21}]Aβ(1-28) is unable to aggregate into β sheets and cytotoxic amyloid. Moreover, cyclo^{17,21}-[Lys^{17}, Asp^{21}]Aβ(1-28) is shown to interact with Aβ(1-28) and to inhibit amyloid formation and cytotoxicity of Aβ(1-28). Cyclo^{17,21}-[Lys^{17}, Asp^{21}]Aβ(1-28) was also shown to be able to interact with Aβ(1-40) and interfere with its amyloidogenesis pathway. These results show for the first time that the direct conformational restriction of the amyloid core of an amyloidogenic sequence via cyclization may lead to an inhibitor of amyloidogenesis and related cytotoxicity. Cyclo^{17,21}-[Lys^{17}, Asp^{21}]Aβ(1-28) and other accordingly modified conformationally constrained Aβ analogs may be suitable candidates or lead compounds for therapeutic or diagnostic approaches in AD.

Experimental Procedures

Materials

Protected amino acids, resins for peptide synthesis, and coupling reagents were from Bachem (Heidelberg, Germany), Rapp Polymere (Tübingen, Germany), Novabiochem (Bad Soden, Germany), and Advanced ChemTech (Louisville, KY). Solvents and chemicals for syntheses, RP-HPLC purifications, and CD studies were from Merck (Darmstadt, Germany) and Aldrich (Deisenhofen, Germany) and were of the highest purity grade available. Synthetic Aβ(1-28) and Aβ(1-40) were from Bachem.

Peptide Synthesis, Purification, and Characterization

Cyclo^{17,21}-[Lys^{17}, Asp^{21}]Aβ(1-28) was synthesized by Boc- and Fmoc-solid phase synthetic protocols essentially as previously described [43, 64, 65]. Crude cyclo^{17,21}-[Lys^{17}, Asp^{21}]Aβ(1-28) was purified by RP-HPLC on a Nucleosil 100 C-18 semipreparative column (100 Å pore size, 7 μm particle size, 8 × 250 mm) (Grom, Herrenberg, Germany) or a Vydac C-4 column (300 Å pore size, 100 μm particle size, 10 × 250 mm) as described [64]. HPLC-purified peptide was characterized by matrix-assisted laser desorption mass spectroscopy (MALDI-MS) which gave MH+ 3306.0 for the peptide synthesized by the Boc strategy and MH+ 3305.3 (calculated 3304.5) for the peptide synthesized by the Fmoc strategy. [Lys^{17}, Asp^{21}]Aβ(1-28) was synthesized using Boc-synthetic protocols and purified as described above. MALDI-MS gave MH+ of 3325.1 (calculated 3322.5). N-terminally biotinylated cyclo^{17,21}-[Aca^{0}, Lys^{17}, Asp^{21}]Aβ(1-28) was synthesized by the Fmoc strategy and purified as above. ε-aminocaproic acid (Aca) was used as a spacer for biotin. MALDI-MS gave MH+ of 3642.3 (calculated 3644.0).

AFM

Peptides were incubated at 2 mM in aqueous 10% HAc for 6 days at room temperature [49]. Following neutralization with aqueous 10% ammonium hydroxide, incubations continued for 2 months at 4°C. Sample preparation and AFM with an AUTOPROBE CP Microscope (Park Scientific Instruments, Sunnyvale, CA) were performed as described [49]. Scanning parameters were drive amplitude between 5 and 6V and scan rate 1.5 Hz. Diameters of the fibrils and dimensions of the aggregates were determined as described [49, 52].

Congo Red Staining

5 μl of aged peptide solutions (2 mM peptide in 10% HAc; 6 days incubation at room temperature; neutralization with 10% ammonium hydroxide) were allowed to air dry on a glass microscope slide, and staining was performed by saturated CR solution in 80% ethanol [51]. Birefringence was determined with an OLYMPUS CK40 light microscope (Olympus, Tokyo, Japan) under cross-polarized light.

FT-IR Spectroscopy

5 μl of aged peptide solutions (incubation as for AFM) were applied onto a CaF_2 plate, air dried, and spectra measured in a Perkin-Elmer spectrophotometer (Spectrum 1000) as described [51].

Aggregation Assays Using EM

Incubations of peptides were performed in assay buffer that consisted of 70% (v/v) sterile-filtered (0.22 μm) 10 mM sodium phosphate buffer, pH 5.5, containing 100 mM NaCl and 30% (v/v) ACN for several days at room temperature. At the indicated time points, 5–20 μl aliquots of solutions/suspensions of the aggregation assays were applied onto formvar/carbon-coated copper grids, stained with uranyl acetate [51], and examined with a Zeiss EM 109 electron microscope operated at 80kV or with a Philips EM 400 T electron microscope operated at 60kV.

CD Spectroscopy

A Jasco J-720 spectropolarimeter was used. Far-UV CD spectra were collected between 195 or 200 and 250 nm, at 0.1 nm intervals, with a response time of 8 s and at room temperature. For the study of amyloidogenesis-related transitions and peptide-inhibitor interactions, the assay buffer was as for EM, and peptide concentrations were 225 and 450 μM. For the determination of the α-helical propensities, peptide concentrations of 5 μM were applied, and the assay buffer consisted of 10% TFE in 10 mM sodium phosphate buffer, pH 3.0. These conditions have been previously shown to correspond to very weak monomeric α helix-promoting conditions for Aβ(1-28) [19] and should allow for the detection of a potential difference between the α-helical propensities of the peptides. Of note, α helix formation has been also found to not depend on the peptide concentration up to the upper micromolar range [19].

Peptide Binding Studies

Aβ(1-40) (10 μg) was incubated alone or with N$^{\alpha}$-biotinyl-cyclo^{17,21}-[Aca^{0}, Lys^{17}, Asp^{21}]Aβ(1-28) (10 μg) in 1 ml phosphate-buffered saline (PBS) for 1 hr. N$^{\alpha}$-biotinyl-cyclo^{17,21}-[Aca^{0}, Lys^{17}, Asp^{21}]Aβ(1-28) (10 μg) was also incubated alone. Streptavidin-coupled magnetic beads (Dynabeads M-280 Streptavidin, Dynal Biotec ASA, Oslo, Norway) (100 μl) were washed with PBS, a solution of 20 mM Tris, pH 7.3, containing 150 mM NaCl and 0.05% Tween 20 (TBSn), and blocked with 0.25% bovine serum albumin (analysis grade) in TBSn overnight. Incubations of the peptides with the beads were performed then for 90 min and bead-bound complexes were isolated by magnetic affinity. Beads were washed with 25 mM HEPES, pH 7.7, containing 0.1 M NaCl and 0.5% Triton X100, reducing NuPAGE sample loading buffer was added, the beads were boiled (10 min), and

supernatants containing the eluted complexes were subjected to NuPAGE electrophoresis in 4%–12% Bis-Tris gels with MES running buffer according to the manufacturer's (Invitrogen, Karlsruhe, Germany) recommendations. Equal amounts of peptide (3.3 μg) were loaded. Peptides were blotted onto nitrocellulose using a XCell II Blot Module blotting system (Invitrogen). Aβ(1-40) bound to N^{α}-biotinyl-cyclo^{17,21}-[Aca^{0}, Lys^{17}, Asp^{21}]Aβ(1-28) was revealed by Western blotting using a polyclonal rabbit anti-Aβ(1-40) antibody (Sigma, Deisenhofen, Germany) in combination with peroxidase (POD)-coupled secondary antibody and the Super Signal Duration ECL staining solution (Pierce/KMF, St. Augustin, Germany). Control blots performed to stain N^{α}-biotinyl-cyclo^{17,21}-[Aca^{0}, Lys^{17}, Asp^{21}]Aβ(1-28) were developed with streptavidin-POD. A biotinylated molecular weight marker ranging from 10 to 60 kDa (New England Biolabs Corp., Heidelberg, Germany) was electrophoresed in the same gels.

NuPAGE Polyacrylamide Gel Electrophoresis and Silver Staining

For the oligomerization studies, peptides (10 μg) were freshly dissolved in 5 μl H_2O, NuPAGE sample buffer was added, mixtures were heated at 95°C for 5 min, and peptides were immediately loaded. For the peptide degradation studies, peptides were aged (see under AFM) and prepared for electrophoresis as above. Electrophoresis was performed in 4%–12% NuPAGE gels (see above). Gels were fixed in 20% trichloroacetic acid (TCA) for at least 1 hr and stained with ammonia-silver complexes [66]. Prestained protein size markers ranging from 6.5 to 175 kDa (Invitrogen) and 3 to 52 kDa (New England Biolabs Corp.) were run in the same gels as standard.

Size Exclusion Chromatography

Size exclusion chromatography was performed with a Toyopearl HW 50-S column (Grom) (250 × 8 mm). The elution buffer was 100 mM sodium phosphate, pH 7.4, containing 200 mM NaCl, the flow rate was 0.25 ml/min and detection was at 214 nm. The column was calibrated with proteins and peptides of known molecular weights. Peptides or peptide mixtures (30 μg each) were dissolved in destilled water (300 μl), and 50 μl was applied onto the column at various time points.

Thioflavin T Binding Assay

Aβ(1-40) (10 μg), cyclo^{17,21}-[Lys^{17}, Asp^{21}]Aβ(1-28) (10 μg), or a mixture of both peptides (10 μg each) were incubated in 50 μl of assay buffer (see under EM). 2 μl aliquots of the solutions were then added into 200 μl of a ThT solution (5 μM ThT in PBS), and ThT binding was measured as described [14]. An increase in fluorescence emission at 486 nm following excitation at 450 nm indicated increased amyloid formation [14, 58]. Fluorescence emission was measured with the 1420 Multilabel Counter Victor^{2} (PerkinElmer Life Sciences, Rheinböllen, Germany).

Cytotoxicity Studies

The HTB14 human glioblastoma/astrocytoma cell line was obtained from the American Type Culture Collection. Cells were cultured and plated as described recently [56]. Peptides (450 μM) or peptide mixtures (450 μM each) were aged for 4 days (see under EM) and applied onto the cells at 5–10 μM. The same results were obtained when the incubations were performed in PBS. Incubations of the aged peptide solutions with the cells and determination of cell viability were performed as described [51].

Supplemental Data

Please write to chembiol@cell.com for a PDF. Supplemental data are presented on (1) the studies of the amyloidogenic properties of [Lys^{17}, Asp^{21}]Aβ(1-28); (2) the studies on peptide stability under the incubation conditions for AFM; and (3) the ThT binding studies.

Acknowledgments

We thank H. Brunner and W. Voelter for helpful discussions. We thank M. Bergmann, K. Tenidis, and M. Waldner for HPLC purifications, J. Beck for assistance in the synthesis and purification of the biotinylated peptides, H. Didden for excellent technical assistance, and K. Sweimeh and R. Kayed for contributions to the EM and CD work. We thank S. Stoeva and K. Laib for MALDI-MS. We thank J. Lorenzen and H.-G. Hollweg for advice with the use of the EM instrument. This work was supported by a grant of The Fraunhofer Institute for Interfacial and Biological Engineering (Stuttgart, Germany) to A.K.

Received: June 4, 2002
Revised: January 6, 2003
Accepted: January 22, 2003

References

1. Selkoe, D.J. (2001). Alzheimer's disease: genes, proteins, and therapy. Physiol. Rev. *81*, 741–766.
2. Glenner, G.G., and Wong, C.W. (1984). Alzheimer's disease: initial report of the purification and characterization of a novel cerebrovascular amyloid protein. Biochem. Biophys. Res. Commun. *120*, 885–890.
3. Ida, N., Hartmann, T., Pantel, J., Schröder, J., Zerfass, R., Förstl, H., Sandbrink, R., Masters, C.L., and Beyreuther, K. (1996). Analysis of heterogeneous βA4 peptides in human cerebrospinal fluid and blood by a newly developed sensitive western blot assay. J. Biol. Chem. *271*, 22908–22914.
4. Koo, E.H., Lansbury, P.T., Jr., and Kelly, J.W. (1999). Amyloid diseases: abnormal protein aggregation in neurodegeneration. Proc. Natl. Acad. Sci. USA *96*, 9989–9990.
5. Iversen, L.L., Mortishire-Smith, J., Pollack, S.J., and Shearman, M.S. (1995). The toxicity in vitro of β-amyloid protein. Biochem. J. *311*, 1–16.
6. Shearman, M.S., Ragan, C.I., and Iversen, L.L. (1994). Inhibition of PC12 cell redox activity is a specific, early indicator of the mechanism of β-amyloid-mediated cell death. Proc. Natl. Acad. Sci. USA *91*, 1470–1474.
7. Pike, C.J., Burdick, D., Walencewicz, A.J., Glabe, C.G., and Cotman, C.W. (1993). Neurodegeneration induced by β-amyloid peptides in vitro: the role of peptide assembly state. J. Neurosci. *13*, 1676–1687.
8. Schubert, D., Behl, C., Lesley, R., Brack, A., Dargusch, R., Sagara, Y., and Kimura, H. (1995). Amyloid peptides are toxic via a common oxidative mechanism. Proc. Natl. Acad. Sci. USA *92*, 1989–1993.
9. Lorenzo, A., and Yankner, B.A. (1994). β-amyloid neurotoxicity requires fibril formation and is inhibited by congo red. Proc. Natl. Acad. Sci. USA *91*, 12243–12247.
10. Walsh, D.M., Klyubin, I., Fadeeva, J.V., Cullen, W.K., Anwyl, R., Wolfe, M.S., Rowan, M.J., and Selkoe, D.J. (2002). Naturally secreted oligomers of amyloid β protein potently inhibit hippocampal long-term potentiation in vivo. Nature *416*, 535–539.
11. Findeis, M.A. (2000). Approaches to discovery and characterization of inhibitors of amyloid β-peptide polymerization. Biochim. Biophys. Acta *1502*, 76–84.
12. Gordon, D.J., Sciarretta, K.L., and Meredith, S.C. (2001). Inhibition of β-amyloid(40) fibrillogenesis and disassembly of β-amyloid(40) fibrils by short β-amyloid congeners containing N-methyl amino acids at alternate residues. Biochemistry *40*, 8237–8245.
13. Soto, C., Sigurdsson, E.M., Morelli, L., Kumar, R.A., Castano, E.M., and Frangione, B. (1998). β-sheet breaker peptides inhibit fibrillogenesis in rat brain model of amyloidosis: implications for Alzheimer's therapy. Nat. Med. *4*, 822–826.
14. Ghanta, J., Shen, C., Kiessling, L.L., and Murphy, R. (1996). A strategy for designing inhibitors of β-amyloid toxicity. J. Biol. Chem. *271*, 29525–29528.
15. Solomon, B., Koppel, R., Hanan, E., and Katzav, T. (1996). Monoclonal antibodies inhibit in vitro fibrillar aggregation of the Alzheimer β-amyloid peptide. Proc. Natl. Acad. Sci. USA *93*, 452–455.
16. Hughes, E., Burke, R.M., and Doig, A.J. (2000). Inhibition of toxicity in the β-amyloid peptide fragment β-(25–35) using N-methylated derivatives. J. Biol. Chem. *275*, 25109–25115.
17. Tjernberg, L.O., Näslund, J., Lindquist, F., Johanson, J., Karlström, A., Thyberg, J., Terenius, J., and Nordstedt, C. (1996).

Arrest of β-amyloid fibril formation by a pentapeptide ligand. J. Biol. Chem. *271*, 8545–8548.

18. Barrow, C.J., and Zagorski, M.G. (1991). Solution structures of β peptide and its constituent fragments: relation to amyloid deposition. Science *253*, 179–182.
19. Barrow, C.J., Yasuda, A., Kenny, P.T.M., and Zagorski, M.G. (1992). Solution conformations and aggregational properties of synthetic amyloid β-peptides of Alzheimer's disease. Analysis of circular dichroism spectra. J. Mol. Biol. *225*, 1075–1093.
20. Soto, C., and Frangione, B. (1995). Two conformational states of amyloid β-peptide: implications for the pathogenesis of Alzheimer's disease. Neurosci. Lett. *186*, 115–118.
21. Zagorski, M.G., and Barrow, C.J. (1992). NMR studies of amyloid β-peptides: proton assigments, secondary structure, and mechanism of an α-helix → β-sheet conversion for a homologous, 28-residue, N-terminal fragment. Biochemistry *31*, 5621–5631.
22. Walsh, D.M., Hartley, D.M., Kusumoto, Y., Fezoui, Y., Condron, M.M., Lomakin, A., Benedek, G.B., Selkoe, D.J., and Teplow, D.B. (1999). Amyloid β-protein fibrillogenesis. Structure and biological activity of protofibrillar intermediates. J. Biol. Chem. *274*, 25945–25952.
23. Wood, S.J., Wetzel, R., Martin, J.D., and Hurle, M.R. (1995). Prolines and amyloidogenicity in fragments of the Alzheimer's peptide β/A4. Biochemistry *34*, 724–730.
24. Pallitto, M.M., Ghanta, J., Heinzelman, P., Kiessling, L.L., and Murphy, R.M. (1999). Recognition sequence design for peptidyl modulators of β-amyloid aggregation and toxicity. Biochemistry *38*, 3570–3578.
25. Ma, K., Clancy, E.L., Zhang, Y., Ray, D.G., Wollenberg, K., and Zagorski, M.G. (1999). Residue-specific pKa measurements of the β-peptide and mechanism of pH-induced amyloid formation. J. Am. Chem. Soc. *121*, 8698–8706.
26. Tjernberg, L.O., Callaway, D.J.E., Tjernberg, A., Hahne, S., Lilliehöök, C., Terenius, L., Thyberg, J., and Nordstedt, C. (1999). A molecular model of Alzheimer amyloid β-peptide fibril formation. J. Biol. Chem. *274*, 12619–12625.
27. Wood, S.J., Maleeff, B., Hart, T., and Wetzel, R. (1996). Physical, morphological and functional differences between pH 5.8 and 7.4 aggregates of the Alzheimer's amyloid peptide Aβ. J. Mol. Biol. *256*, 870–877.
28. Esler, W.P., Stimson, E.R., Ghilardi, J.R., Lu, Y.-A., Felix, A.M., Vinters, H.V., Mantyh, P.W., Lee, J.P., and Maggio, J.E. (1996). Point substitution in the central hydrophobic cluster of a human β-amyloid congener disrupts peptide folding and abolishes plaque competence. Biochemistry *35*, 13914–13921.
29. Hilbich, C., Kisters-Woike, B., Reed, J., Masters, C.L., and Beyreuther, K. (1991). Aggregation and secondary structure of synthetic amyloid βA4 peptides of Alzheimer's disease. J. Mol. Biol. *218*, 149–163.
30. Hilbich, C., Kisters-Woike, B., Reed, J., Masters, C.L., and Beyreuther, K. (1992). Substitutions of hydrophobic amino acids reduces the amyloidogenicity of Alzheimer's disease βA4 peptides. J. Mol. Biol. *228*, 460–473.
31. Zhang, S., Iwata, K., Lachenmann, M.J., Peng, J.W., Li, S., Stimson, E.R., Lu, Y.-A., Felix, A.M., Maggio, J.E., and Lee, J.P. (2000). The Alzheimer's peptide Aβ adopts a collapsed coil structure in water. J. Struct. Biol. *130*, 130–141.
32. Kirkitadze, M.D., Condron, M.M., and Teplow, D.B. (2001). Identification and characterization of key kinetic intermediates in amyloid β-protein fibrillogenesis. J. Mol. Biol. *312*, 1103–1119.
33. Kirschner, D.A., Inouye, H., Duffy, L.K., Sinclair, A., Lind, M., and Selkoe, D.J. (1987). Synthetic peptide homologous to β protein from Alzheimer's disease forms amyloid-like fibrils *in vitro*. Proc. Natl. Acad. Sci. USA *84*, 6953–6957.
34. Talafous, J., Marcinowski, K.J., Klopman, G., and Zagorski, M.G. (1994). Solution structure of residues 1–28 of the amyloid β-peptide. Biochemistry *33*, 7788–7796.
35. Fraser, P.E., Nguyen, J.T., Surewicz, W.K., and Kirschner, D.A. (1991). pH-dependent structural transitions of Alzheimer's amyloid peptides. Biophys. J. *60*, 1190–1201.
36. Soto, C., Castano, E.M., Frangione, B., and Inestrosa, N.C. (1995). The α-helical to β-strand transition in the amino-terminal fragment of the amyloid β-peptide modulates amyloid formation. J. Biol. Chem. *270*, 3063–3067.
37. Shen, C.-L., Scott, G.L., Merchant, F., and Murphy, R.M. (1993). Light scattering analysis of fibril growth from the amino-terminal fragment β(1–28) of β-amyloid peptide. Biophys. J. *65*, 2383–2395.
38. Hruby, V.J. (1982). Conformational restrictions of biologically active peptides via amino acid side chain groups. Life Sci. *31*, 189–199.
39. Rizo, J., and Gierasch, L.M. (1992). Constrained peptides: models of bioactive peptides and protein substructures. Annu. Rev. Biochem. *61*, 387–418.
40. Felix, A.M., Heimer, E.P., Wang, C.T., Lambros, T.J., Fournier, A., Mowles, T.F., Maines, S., Campbell, R.M., Wegrzynski, B.B., Toome, V., et al. (1988). Synthesis, biological activity and conformational analysis of cyclic GRF analogs. J. Pept. Res. *32*, 441–454.
41. Felix, A.M., Wang, C.T., Campbell, R.M., Toome, V., Fry, D., and Madison, V.S. (1992). Biologically active cyclic (lactam) analogs of growth hormone-releasing factor: effect of ring size and location on conformation and biological activity. In Peptides, Chemistry and Biology, J.A. Smith and J.E. Rivier, eds. (Leiden, NL: ESCOM Science Publishers), pp. 77–79.
42. Chorev, M., Roubini, E., McKee, R.L., Gibbons, S.W., Goldman, M.E., Caulfield, M.P., and Rosenblatt, M. (1991). Cyclic parathyroid hormone related protein antagonists: lysine 13 to aspartic acid 17 [i to (i+4)] side chain to side chain lactamization. Biochemistry *30*, 5968–5974.
43. Kapurniotu, A., and Taylor, J.W. (1995). Structural and conformational requirements for human calcitonin activity: design, synthesis, and study of lactam-bridged analogs. J. Med. Chem. *38*, 836–847.
44. Taylor, J.W., Jin, Q.K., Sbacchi, M., Wang, L., Belfiore, P., Garnier, M., Kazantzis, A., Kapurniotu, A., Zaratin, P.F., and Scheideler, M.A. (2002). Side-chain lactam-bridge conformational constraints differentiate the activities of salmon and human calcitonins and reveal a new design concept for potent calcitonin analogs. J. Med. Chem. *45*, 1108–1121.
45. Jackson, D.Y., King, D.S., Chmielewski, J., Singh, S., and Schultz, P.G. (1991). General approach to the synthesis of short α-helical peptides. J. Am. Chem. Soc. *113*, 9391–9392.
46. Andreu, D., Albericio, F., Sole, N.A., Munson, M.C., Ferrer, M., and Barany, G. (1994). Formation of disulfide bonds in synthetic peptides and proteins. In Methods in Molecular Biology: Peptide Synthesis Protocols, M.W. Pennington and B.M. Dunn, eds. (Totowa, NJ: Humana Press Inc.), pp. 91–169.
47. Krampert, M., Bernhagen, J., Schmucker, J., Horn, A., Schmauder, A., Voelter, W., Brunner, H., and Kapurniotu, A. (2000). Amyloidogenicity of recombinant human pro-islet amyloid polypeptide (ProIAPP). Chem. Biol. *7*, 855–871.
48. Harper, J.D., and Lansbury, P.T., Jr. (1997). Models of amyloid seeding in Alzheimer's disease and scrapie: mechanistic truths and physiological consequences of the time-dependent solubility of amyloid proteins. Annu. Rev. Biochem. *66*, 385–407.
49. Kayed, R., Bernhagen, J., Greenfield, N., Sweimeh, K., Brunner, H., Voelter, W., and Kapurniotu, A. (1999). Conformational transitions of islet amyloid polypeptide (IAPP) in amyloid formation *in vitro*. J. Mol. Biol. *287*, 781–796.
50. Fraser, P.E., McLachlan, D.R., Surewicz, W.K., Mizzen, C.A., Snow, A.D., Nguyen, J.T., and Kirschner, D.A. (1994). Conformation and fibrillogenesis of Alzheimer Aβ peptides with selected substitution of charged residues. J. Mol. Biol. *244*, 64–73.
51. Tenidis, K., Waldner, M., Bernhagen, J., Fischle, W., Bergmann, M., Weber, M., Merkle, M.-L., Voelter, W., Brunner, H., and Kapurniotu, A. (2000). Identification of a penta- and hexapeptide of islet amyloid polypeptide (IAPP) with amyloidogenic and cytotoxic properties. J. Mol. Biol. *295*, 1055–1071.
52. Stine, W.B., Jr., Snyder, S.W., Ladror, U.S., Wade, W.S., Miller, M.F., Perun, T.J., Holzman, T.F., and Krafft, G.A. (1996). The nanometer-scale structure of amyloid-β visualized by atomic force microscopy. J. Protein Chem. *15*, 193–202.
53. Sunde, M., and Blake, C. (1997). The structure of amyloid fibrils by electron microscopy and x-ray diffraction. Adv. Protein Chem. *50*, 129–159.
54. Krimm, S., and Bandekar, J. (1986). Vibrational spectroscopy

and conformation of peptides, polypeptides, and proteins. Adv. Protein Chem. *38*, 181–364.

55. Woody, R.W. (1985). Circular dichroism of peptides. In The peptides, Analysis, Synthesis, Biology, S. Udenfriend, J. Meienhofer, and V. Hruby, eds. (New York: Academic Press), pp. 15–114.
56. Kapurniotu, A., Schmauder, A., and Tenidis, K. (2002). Structure-based design and study of non-amyloidogenic, double N-methylated IAPP amyloid core sequences as inhibitors of IAPP amyloid formation and cytotoxicity. J. Mol. Biol. *315*, 339–350.
57. Kleemann, R., Hausser, A., Geiger, G., Mischke, R., Burger-Kentischer, A., Flieger, O., Johannes, F.-J., Roger, T., Calandra, T., Kapurniotu, A., et al. (2000). Intracellular action of the cytokine MIF to modulate AP-1 activity and the cell cycle through Jab1. Nature *408*, 211–216.
58. LeVine, H.I. (1993). Thioflavine T interaction with synthetic Alzheimer's disease β-amyloid peptides: detection of amyloid aggregation in solution. Protein Sci. *2*, 404–410.
59. Esler, W.P., Felix, A.M., Stimson, E.R., Lachenmann, M.J., Ghilardi, J.R., Lu, Y.-A., Vinters, H.V., Mantyh, P.W., Lee, J.P., and Maggio, J.E. (2000). Activation barriers to structural transition determine deposition rates of Alzheimer's disease Aβ amyloid. J. Struct. Biol. *130*, 174–183.
60. Kapurniotu, A., Bernhagen, J., Greenfield, N., Al-Abed, Y., Teichberg, S., Frank, R.W., Voelter, W., and Bucala, R. (1998). Contribution of advanced glycosylation to the amyloidogenicity of islet amyloid polypeptide. Eur. J. Biochem. *251*, 208–216.
61. Judice, J.K., Tom, J.Y.K., Huang, W., Wrin, T., Vennari, J., Petropoulos, C.J., and McDowell, R.S. (1997). Inhibition of HIV type 1 infectivity by constrained α-helical peptides: implications for the viral fusion mechanism. Proc. Natl. Acad. Sci. USA *94*, 13426–13430.
62. Walsh, D.M., Lomankin, A., Benedek, G.B., Condron, M.M., and Teplow, D.B. (1997). Amyloid β-protein fibrillogenesis. Detection of a protofibrillar intermediate. J. Biol. Chem. *272*, 22364–22372.
63. Lambert, M.P., Barlow, A.K., Chromy, B.A., Edwards, C., Freed, R., Liosatos, M., Morgan, T.E., Rozovsky, I., Trommer, B., Viola, K.L., et al. (1998). Diffusible, nonfibrillar ligands derived from $A\beta_{1-42}$ are potent central nervous system neurotoxins. Proc. Natl. Acad. Sci. USA *95*, 6448–6453.
64. Kapurniotu, A., Kayed, R., Taylor, J.W., and Voelter, W. (1999). Rational design, confomational studies and bioactivity of novel, highly potent, conformationally constrained calcitonin analogs. Eur. J. Biochem. *265*, 606–618.
65. Kazantzis, A., Waldner, M., Taylor, J.W., and Kapurniotu, A. (2002). Conformationally constrained human calcitonin (hCt) analogs reveal a critical role of sequence 17–21 for the oligomerization state and bioactivity of hCt. Eur. J. Biochem. *269*, 780–791.
66. Kleemann, R., Kapurniotu, A., Mischke, A., Held, J., and Bernhagen, J. (1999). Characterization of catalytic center mutants of macrophage migration inhibitory factor (MIF) and comparison to C81S MIF. Eur. J. Biochem. *261*, 753–766.